



**British
Geological Survey**
Expert | Impartial | Innovative

Ground Motion and Stratum Thickness Comparison in Tower Hamlets, London

Engineering Geology and Infrastructure Programme

Open Report OR/19/043

BRITISH GEOLOGICAL SURVEY

ENGINEERING Geology and Infrastructure Programme

OPEN REPORT OR/19/043

Ground Motion and Stratum Thickness Comparison in Tower Hamlets, London

A Novellino, R Terrington, V Christodoulou, H Smith & L Bateson

The National Grid and other
Ordnance Survey data © Crown
Copyright and database rights
2018. Ordnance Survey Licence
No. 100021290 EUL.

Keywords

Report; Tunnelling, ground
deformation, InSAR.

Bibliographical reference

NOVELLINO, A, TERRINGTON, R,
CHRISTODOULOU, V, SMITH, H,
BATESON, L 2019.
Ground Motion and Stratum
Thickness Comparison in Tower
Hamlets, London. *British
Geological Survey Open Report*,
OR/19/043. 31pp.

Copyright in materials derived
from the British Geological
Survey's work is owned by
UK Research and Innovation
(UKRI) and/or the authority that
commissioned the work. You may
not copy or adapt this publication
without first obtaining permission.
Contact the BGS Intellectual
Property Rights Section, British
Geological Survey, Keyworth,
e-mail ipr@bgs.ac.uk. You may
quote extracts of a reasonable
length without prior permission,
provided a full acknowledgement
is given of the source of the
extract.

Maps and diagrams in this book
use topography based on Ordnance
Survey mapping.

BRITISH GEOLOGICAL SURVEY

The full range of our publications is available from BGS shops at Nottingham, Edinburgh, London and Cardiff (Welsh publications only) see contact details below or shop online at www.geologyshop.com

The London Information Office also maintains a reference collection of BGS publications, including maps, for consultation.

We publish an annual catalogue of our maps and other publications; this catalogue is available online or from any of the BGS shops.

The British Geological Survey carries out the geological survey of Great Britain and Northern Ireland (the latter as an agency service for the government of Northern Ireland), and of the surrounding continental shelf, as well as basic research projects. It also undertakes programmes of technical aid in geology in developing countries.

The British Geological Survey is a component body of UK Research and Innovation.

British Geological Survey offices

**Environmental Science Centre, Keyworth, Nottingham
NG12 5GG**

Tel 0115 936 3100

BGS Central Enquiries Desk

Tel 0115 936 3143

email enquiries@bgs.ac.uk

BGS Sales

Tel 0115 936 3241

email sales@bgs.ac.uk

**The Lyell Centre, Research Avenue South, Edinburgh
EH14 4AP**

Tel 0131 667 1000

email scotsales@bgs.ac.uk

Natural History Museum, Cromwell Road, London SW7 5BD

Tel 020 7589 4090

Tel 020 7942 5344/45 email bgs london@bgs.ac.uk

**Cardiff University, Main Building, Park Place, Cardiff
CF10 3AT**

Tel 029 2167 4280

**Macleon Building, Crowmarsh Gifford, Wallingford
OX10 8BB**

Tel 01491 838800

**Geological Survey of Northern Ireland, Department of
Enterprise, Trade & Investment, Dundonald House, Upper
Newtownards Road, Ballymiscaw, Belfast, BT4 3SB**

Tel 01232 666595

www.bgs.ac.uk/gsni/

**Natural Environment Research Council, Polaris House,
North Star Avenue, Swindon SN2 1EU**

Tel 01793 411500

Fax 01793 411501

www.nerc.ac.uk

**UK Research and Innovation, Polaris House, Swindon
SN2 1FL**

Tel 01793 444000

www.ukri.org

Website www.bgs.ac.uk

Shop online at www.geologyshop.com

Foreword

This report is the published product of a study by the British Geological Survey (BGS) as part of the Engineering Geology and Infrastructure Programme. The study forms part of the wider investigations into anthropogenic deposits (character and distribution) in the Urban Geoscience team.

Contents

Foreword	1
Contents	1
Summary	4
1 Introduction	5
1.1 Artificially Modified Ground	6
1.2 London and the Thames Valley Geological Model	8
2 Methodology	13
3 Results	17
4 Discussion and Conclusions	24
5 Acknowledgments	25
References	26

FIGURES

Figure 1. Spatial coverage of the 3D geological model of London and the Thames Valley with indication of the administrative boundary of the London Borough of Tower Hamlets. Contains Ordnance Data © Crown Copyright and database rights 2019. Ordnance Survey Licence no. 100021290.....	6
Figure 2. AMG thickness map for the Tower Hamlets area. Contains Ordnance Data © Crown Copyright and database rights 2019. Ordnance Survey Licence no. 100021290.....	8
Figure 3. Geological model of London and the Thames Valley.	9
Figure 4. Map showing the uppermost natural geological unit present immediately beneath the AMG from three perspectives: looking toward NE (top), SE (middle) and NW (bottom).	12
Figure 5. Thickness map in the AoI after removal of the AMG thickness (see Figure 2) for ALV (a), RTDU (b), LASI (c), KPGR (d), TPGR (e), HAGR (f), LC (g), LMBE (h) and TAB (i). Contains Ordnance Data © Crown Copyright and database rights 2019. Ordnance Survey Licence no. 100021290.....	13
Figure 6. Vertical velocity measured by Sentinel-1 data during the period 2015 to 2018 across Greater London and the AOI (in red). Positive values indicate uplift and negative values indicate subsidence. InSAR data © CGG NPA Satellite Mapping 2018. Contains modified Copernicus Sentinel data 2014-2018. Contains Ordnance Data © Crown Copyright and database rights 2019. Ordnance Survey Licence no. 100021290.....	14
Figure 7. LOS velocity measured by Sentinel-1 data during the period 2015 to 2017 across Tower Hamlets (in black). Positive values indicate uplift and negative values indicate subsidence. InSAR data © CGG NPA Satellite Mapping 2019. Contains modified Copernicus Sentinel data 2014-2018. Contains Ordnance Data © Crown Copyright and database rights 2019. Ordnance Survey Licence no. 100021290.....	17
Figure 8. Comparison of MP average velocity with thickness of: AMG (a), ALV (b), RTDU (c), LASI (d), KPGR (e), TPGR (f), HAGR (g), LC (h), LMBE (i), TAB (j). The correlation coefficient values (ρ) are provided (top right).....	18
Figure 9. The elbow graph produced from clustering the Tower Hamlets dataset.	19
Figure 10. The spatial pattern of the shape-based distance cluster analysis. The solid curves show the centroids (median) of the distribution of the five clusters. The shaded area denotes the standard deviation ± 1 of each of the size bins, for all distributions that were members of the given clusters. Note the Y-axis has been scaled for each plot independently to highlight the differences within the plot.	21
Figure 11. Comparison of clustering trends with thickness of: AMG (a), ALV (b), RTDU (c), LASI (d), KPGR (e), TPGR (f), HAGR (g), LC (h), LMBE (i), TAB (j). On each box, the central mark indicates the median, and the bottom and top edges of the box indicate the 25 th and 75 th percentiles, respectively. The whiskers extend to the most extreme data points not considering outliers. Outliers are plotted using the red '+' symbol if they lie between 1.5 and 3 times the interquartile range or the red 'o' symbol if they lie outside 3 times the interquartile range. Box width is proportional to the number of samples within each cluster.....	22
Figure 12. Distribution of median and IQR values of the cluster groups for each unit, after the normalization of the thickness values.....	23

Figure 13. Distribution of clustering groups in Tower Hamlets area (a) and groundwater level increase between August 2015 and May 2016 (b). Borehole data used for interpolating the groundwater levels have been provided with the permissions of Canary Wharf Contractors, Crossrail Ltd, Environment Agency and Thames Water. These reproduced materials are courtesy of Crossrail Ltd. Contains Ordnance Data © Crown Copyright and database rights 2019. Ordnance Survey Licence no. 100021290..... 23

TABLES

Table 1. Summary of the superficial and bedrock units underlying the AMG within the AoI following their stratigraphic order, from top to bottom. The Lexicon code database provides BGS definitions of named rock units as they appear on our maps and in our publications (see https://www.bgs.ac.uk/lexicon/home.html).....	10
Table 2. Number of MPs falling into each units ordered from the top to the bottom according to the local stratigraphy.	18
Table 3. The second derivative of each point from the graph shown in Figure 9.....	20

Summary

This report is the published product of a study by the British Geological Survey (BGS) to identify the impact of thickness and distribution of different strata beneath the borough of Tower Hamlets in London compared against temporal ground motion resulting from anthropogenic activities. Other units which are known to have potential high shrink and swelling characteristics in this location were also considered.

Focus was on a newly developed Artificially Modified Ground (AMG) 3D layer where the thickness and distribution was calculated using boreholes and landuse types. The layer has been used to refine the thickness of the other lithological units in the area.

Ground motion data for the 2015-2018 period was derived using spaceborne Interferometric Synthetic Aperture Radar (InSAR) which can measure surface displacement to millimetre accuracy in urban areas. A machine learning technique, called cluster analysis, has been used to group ground motion pattern of 23,245 points within the borough in space and time. The relationship with the thickness of the AMG and the underlying superficial and bedrock units was then studied.

The results show that, within the area of study, the main component of motion is the uplift connected, in time, with the underground anthropogenic activities in the area. Ground displacement patterns are not connected with the thickness of the thickest and deepest units (London Clay, Lambeth Group and Thanet Formation) but have a connection to the most superficial deposits (Alluvium, River Terrace Deposits, Langley Silt Member and Kempton Park Gravel Member).

1 Introduction

Urban areas are covered with a multitude of different types of artificially modified ground (AMG) which vary in character and geometry (Bridge et al, 2005, Bridge et al., 2010, Price et al., 2012, Burke et al., 2014). AMG have been mapped and studied extensively by the BGS, particularly as they impact on areas where there tends to be a large human population. Understanding the geometries and character of the AMG, and the interaction with underlying bedrock units improves the way in which the land is utilised for further development and how hazards, such as subsidence and uplift, are mitigated. Vertical motion is a major geological hazard that affects the stability of foundations and deep basements of buildings with the Association of British Insurers estimating that the average cost of shrink–swell-related subsidence to the insurance industry stands at over £400 million a year.

In London, the London Clay has long been known as a major contributor to subsidence and uplift due its inherent characteristics for shrinking and swelling (Jones, 2011) which is affected by groundwater levels. The water table in London has risen up to 15 m since 2000 despite the London Licensing Strategy encouraging abstraction in areas of the aquifer where the pressure head is in the London Clay (Environment Agency - EA, 2018).

This study aims to identify any lithological control on the ground deformation detected by Interferometric Synthetic Aperture Radar (InSAR) and related to groundwater level changes.

The thickness and geometries of AMG and underground deposits derived from the London and Thames Valley 3D geological model have been considered as lithological parameters.

The Area of Interest (AoI) for this study is the London Borough of Tower Hamlets (Figure 1) because:

- An AMG thickness map was constructed there just prior to this study thanks to the availability of 6,353 boreholes in the 19,77 km² occupied by the AoI.
- The London and Thames Valley London Lithoframe 50 model covers this area so the underlying modelled unit thicknesses and geometries could be considered (Burke et al, 2014). The London Basin 1:50,000 resolution 3D geological model covers a total area of 4,800 km² in southeast England, from easting 450,000 to 570,000 and from northing 160,000 to 200,000 (Figure 1).
- InSAR ground motion data available back to 1992 has already shown that, historically, this area strongly undergoes ground elevation changes on short temporal scales (Cigna et al., 2015).

- *Disturbed Ground*: areas of surface or near-surface mineral workings where ill-defined excavations, areas of subsidence caused by workings, and spoil are complexly related. This is mainly associated with brickearth workings in the study area, but these deposits have been commonly buried by subsequent development and are now shown as Made Ground;
- *Landscaped Ground*: areas where the pre-existing land surface has been extensively remodelled but where it is impracticable to delineate separate areas of Made Ground, Worked Ground or Disturbed Ground. Landscaped Ground is not explicitly shown on published 1:50 000 scale geological maps of the area, with the exception of small areas of industrial development in Tower Hamlets, but is likely to be more extensive in areas where Made Ground is not observed.

Recent progress made by BGS and others around the world in this field has meant that AMG is increasingly mapped and modelled, and is now regarded by many as an important deposit or excavation likened to natural geological processes (Bridge et al., 2005; Bridge et al., 2010; Burke et al., 2014; Price et al., 2012; Zalasiewicz et al., 2011). Boreholes are an important resource for mapping the geometry and character of AMG, as these records preserve former landscape evolution inferring the thickness change from previous land levels and the start heights of boreholes (Terrington et al, 2018), and help indicate current thicknesses of AMG using logged core (Terrington et al, 2015).

The data, methods and processes used to calculate the thickness of the AMG are a continuation of those used in the Terrington *et al* work of 2018. This involved the following steps:

- Deriving the maximum thickness of each borehole log that has recorded AMG in the BGS Borehole Geology and Geotechnical databases.
- For those borehole logs without AMG recorded, the start height (height at which drilling was commenced and a measured ground level) was used as a proxy for land surface elevation change against a modern Digital Terrain Model (DTM) from which a pseudo thickness value could be calculated. For some areas negative values occurred for the thickness, which is where the modern DTM would show Worked Ground when measuring against the historical start height of a borehole. For those areas showing positive thickness values, this indicates areas of Made Ground or potentially even Worked and Made Ground.
- The results of the above were used to calculate a thickness map using ArcGIS using both Inverse Distance Weighting and Kriging functions and assess which is most suited to give 'reasonable' values.

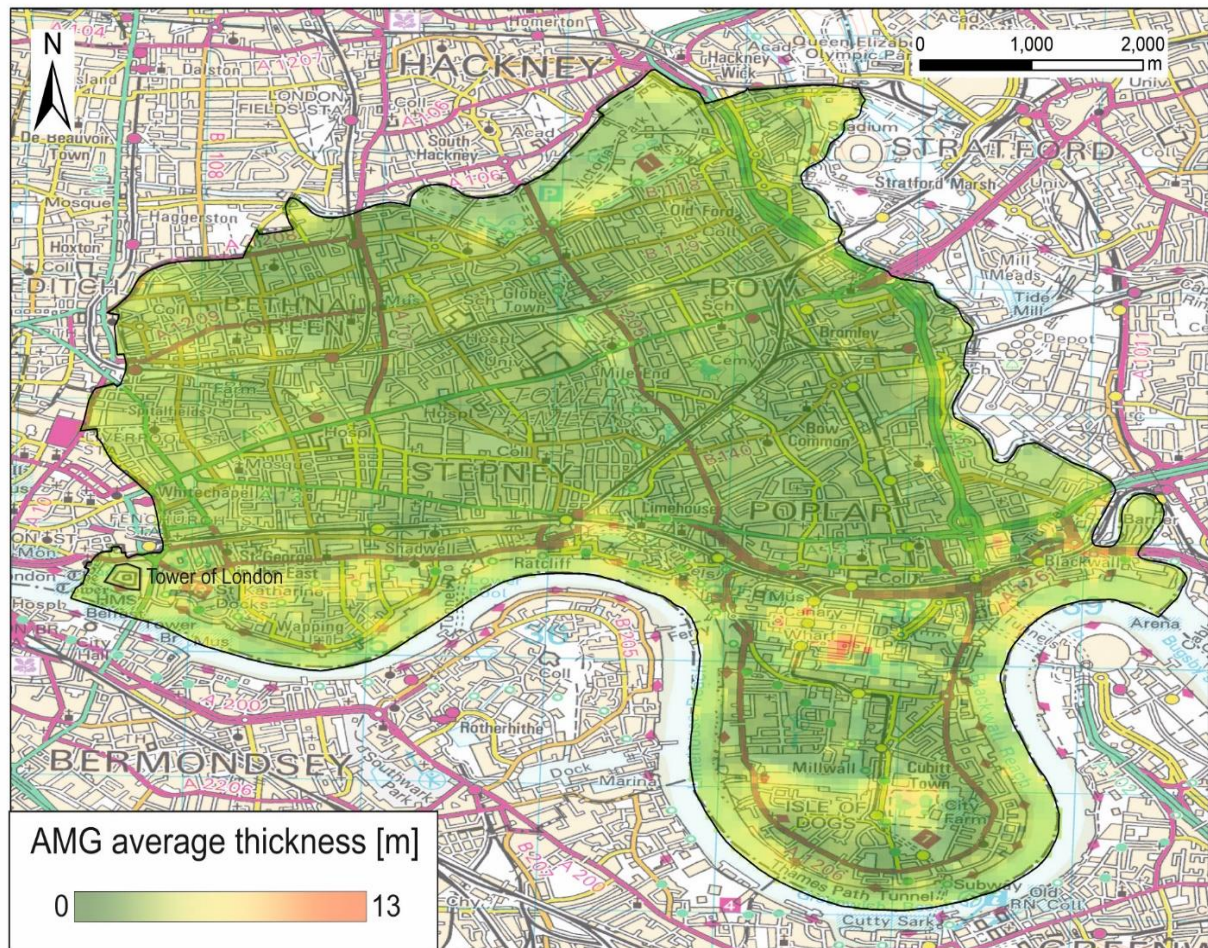


Figure 2. AMG thickness map for the Tower Hamlets area. Contains Ordnance Data © Crown Copyright and database rights 2019. Ordnance Survey Licence no. 100021290.

Around 54.8 million m^3 of AMG characterize the AoI with the spatial distribution of the deposit controlled by the proximity to the River Thames and variation in underlying geology with the highest values usually in the southern part of the AoI (Terrington et al., 2018).

AMG distribution in Tower Hamlets has a large variety of historical landuse and building types spanning from buildings of exceptional national interest (e.g. the Tower of London, Tower Bridge and Christ Church Spitalfields) and recent commercial/residential infrastructures following the closure of London's docks in the 1960s and regeneration of dormant land began in earnest in the 1980s.

1.2 LONDON AND THE THAMES VALLEY GEOLOGICAL MODEL

The geological model for the units underlying the AMG was constructed using the GSI3D software and methodology (Kessler & Mathers 2004, Kessler et al. 2009). The superficial units were calculated in GSI3D, while the bedrock units were calculated in GOCAD using the Structural Modelling workflow as these were faulted structures. This model is intended for use at scales around 1:50,000, together with the corresponding DiGMapGB-50 geological map data. This model is not recommended for site specific studies or use, but gives a wider city to regional scale appreciation of geological structure and geomorphology (Figure 3).

In total, 64 superficial and artificial geological units were modelled (including mass movement deposits) for the London and Thames Valley Model from the surface to a maximum depth of several hundred meters (Figure 3). AMG was mapped in the model in 2D, but was excluded from the model calculation because there was insufficient data to constrain the base of these deposits

(the Z elevation) and so produce a calculated volume. Hence AMG was calculated separately (section 1.1). In total, 7174 borehole logs were considered, comprising both confidential and open access borehole data, plus geotechnical boreholes that were absent from the BGS Single Onshore Borehole Index (SOBI) and 922 cross-sections were constructed across the area of varying lengths and detail.

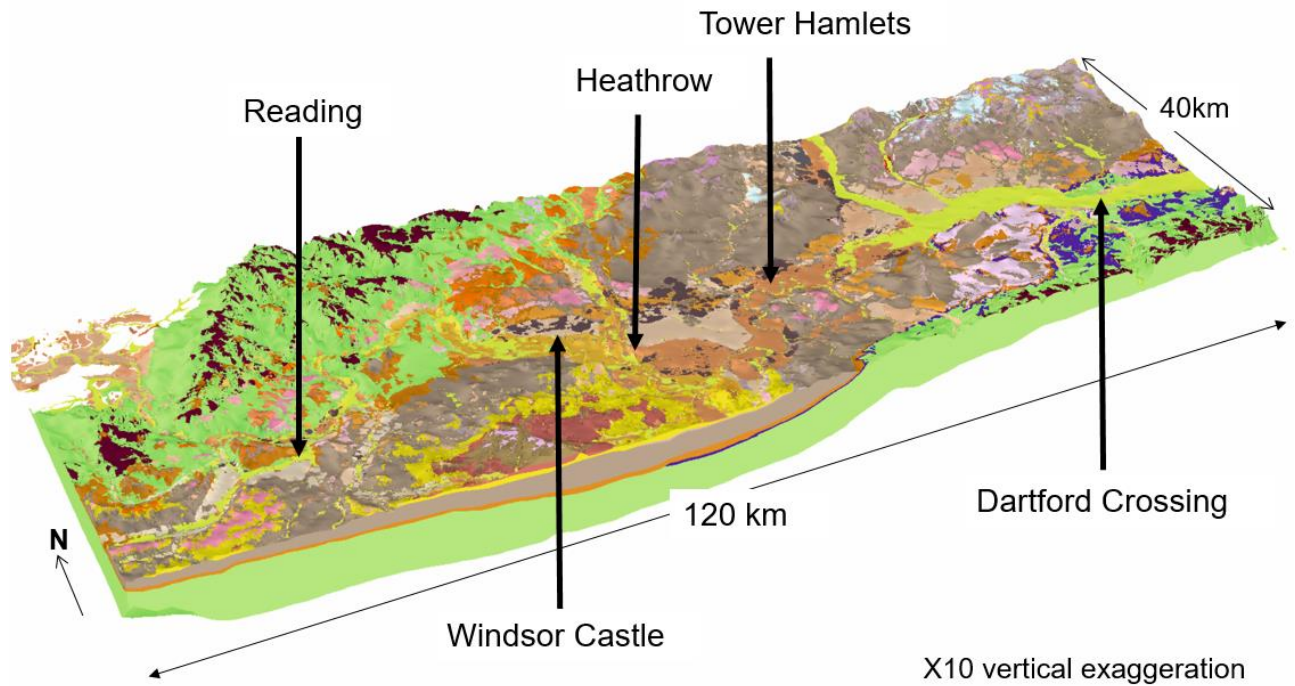


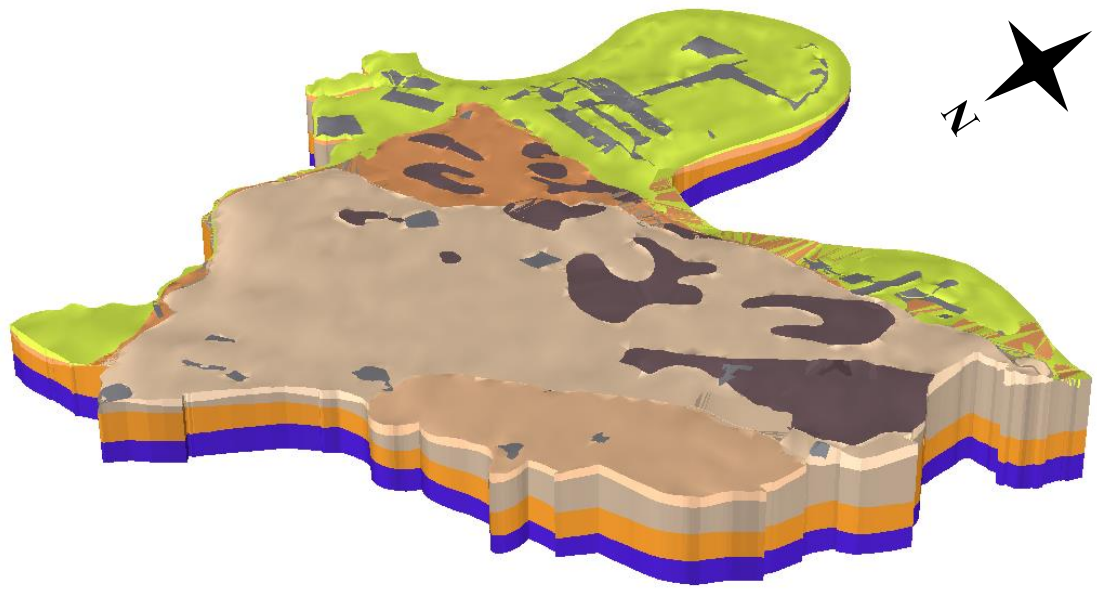
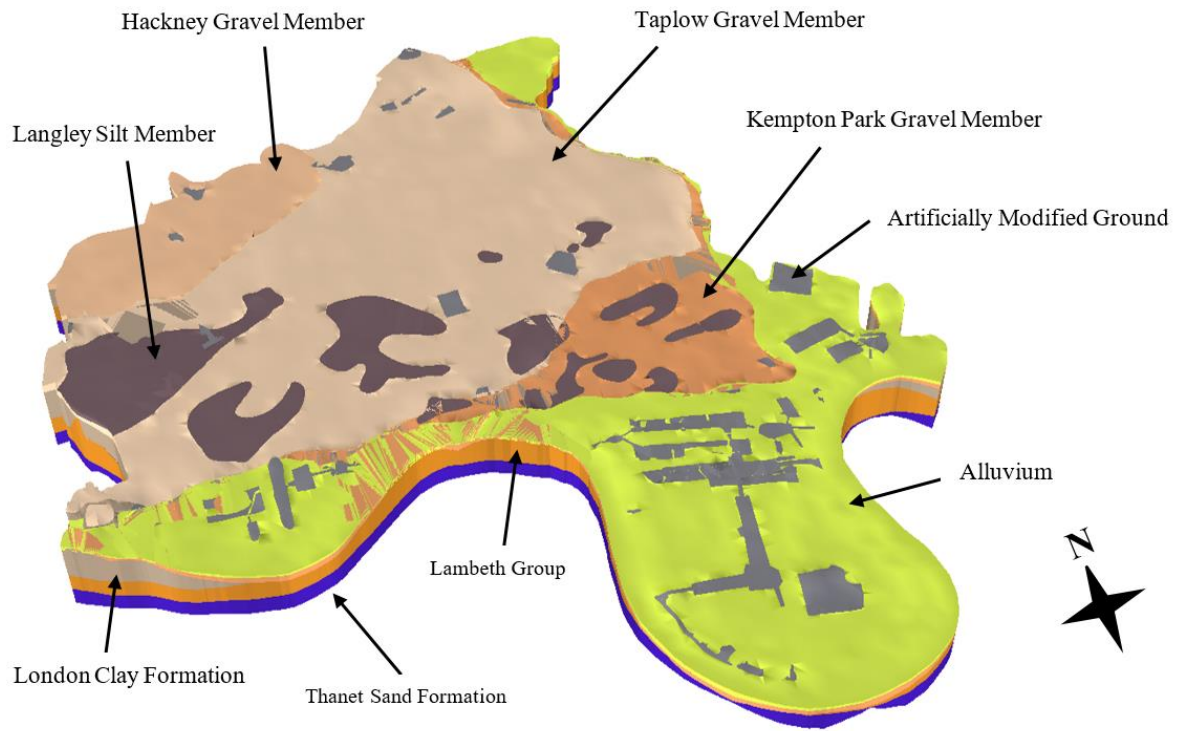
Figure 3. Geological model of London and the Thames Valley.

In the Borough of Tower Hamlets, the following superficial and bedrock units are present and were used in the comparison of the AMG thickness against the InSAR derived ground motion data (Table 1). Conventionally, superficial deposits are the youngest geological deposits formed during the most recent period of geological time, the Quaternary, which extends back about 2.6 million years from the present. They rest on older deposits or rocks referred to as bedrock.

Table 1. Summary of the superficial and bedrock units underlying the AMG within the AoI following their stratigraphic order, from top to bottom. The Lexicon code database provides BGS definitions of named rock units as they appear on our maps and in our publications (see <https://www.bgs.ac.uk/lexicon/home.html>).

Inferred Age	Lexicon code	Full Name – category	Lithology
Holocene	ALV	Alluvium - superficial	Fluvial deposits of modern flood plains, consisting of clay, silt, sand and peat
Late Anglian – Devensian glacial and river terraces	RTDU	River Terrace Deposits (undifferentiated) - superficial	Sand and gravel deposits directly beneath alluvium
Late Anglian – Devensian glacial and river terraces	LASI	Langley Silt Member - superficial	Varies from silt to clay, usually yellow brown and massively bedded
Late Anglian – Devensian glacial and river terraces	KPGR	Kempton Park Gravel Member - superficial	Sand and gravel, with local lenses of silt, clay or peat
Late Anglian – Devensian glacial and river terraces	TPGR	Taplow Gravel Member - superficial	Sand and gravel, locally with lenses of silt, clay or peat
Late Anglian – Devensian glacial and river terraces	HAGR	Hackney Gravel Member - superficial	Sand and gravel, locally with lenses of silt, clay or peat
Eocene	LC	London Clay Formation - bedrock	Bioturbated or poorly laminated, blue-grey or grey-brown, slightly calcareous, silty to very silty clay
Eocene	LMBE	Lambeth Group - bedrock	Vertically and laterally variable sequences mainly of clay, some silty or sandy, with some sands and gravels, minor limestones and lignites and occasional sandstone and conglomerate.
Eocene	TAB	Thanet Formation - bedrock	Glauconite-coated, nodular flint at base, overlain by pale yellow-brown, fine-grained sand that can be clayey and glauconitic. Rare calcareous or siliceous sandstones.

The alluvial deposits dominate the surface the near subsurface in the south of the AoI, and range between 1 and 9 m in thickness. Terrace gravels and Langley Silt member dominate the remainder of the northern half of the AoI. Both the London Clay Formation and Lambeth Group are thinning to outcrop in the south of the area, and becoming thicker and deeper to the north. The London Clay Formation averages 14 m in thickness, and at its thickest point in Tower Hamlets it is 30-35 m. The Lambeth Group averages 16.5 m in thickness, and at its thickest point is ~45 m (Figure 4). HAGR, RTDU and TPGR have the most heterogeneity in thickness.



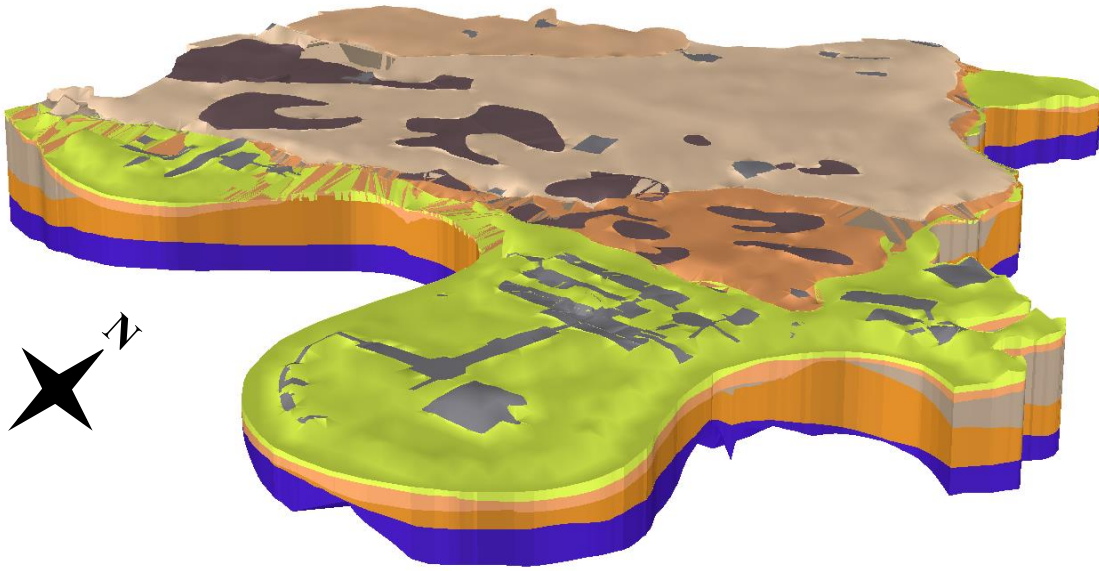


Figure 4. Map showing the uppermost natural geological unit present immediately beneath the AMG from three perspectives: looking toward NE (top), SE (middle) and NW (bottom).

2 Methodology

The newly defined AMG layer has been used as the model cap to adjust the thicknesses of the Lithoframe 50 model within the Tower Hamlets Borough where, on the other hand, values have been calculated considering the DTM as the model cap (Figure 5).

While superficial units (ALV – Figure 5a, RTDU – Figure 5b, LASI – Figure 5c, KPGR – Figure 5d, TPGR – Figure 5e, HAGR Figure 5f) tend to be very limited in spatial extent and of limited thickness (≤ 5 m), deeper units (LC Figure - 5g, LMBE - Figure 5h and TAB - Figure 5i) tend to cover a larger area and be thicker on average (≥ 10 m).

As the calculation of the thickness was completed using GSI3D, the thicknesses across this fault were calculated accurately.

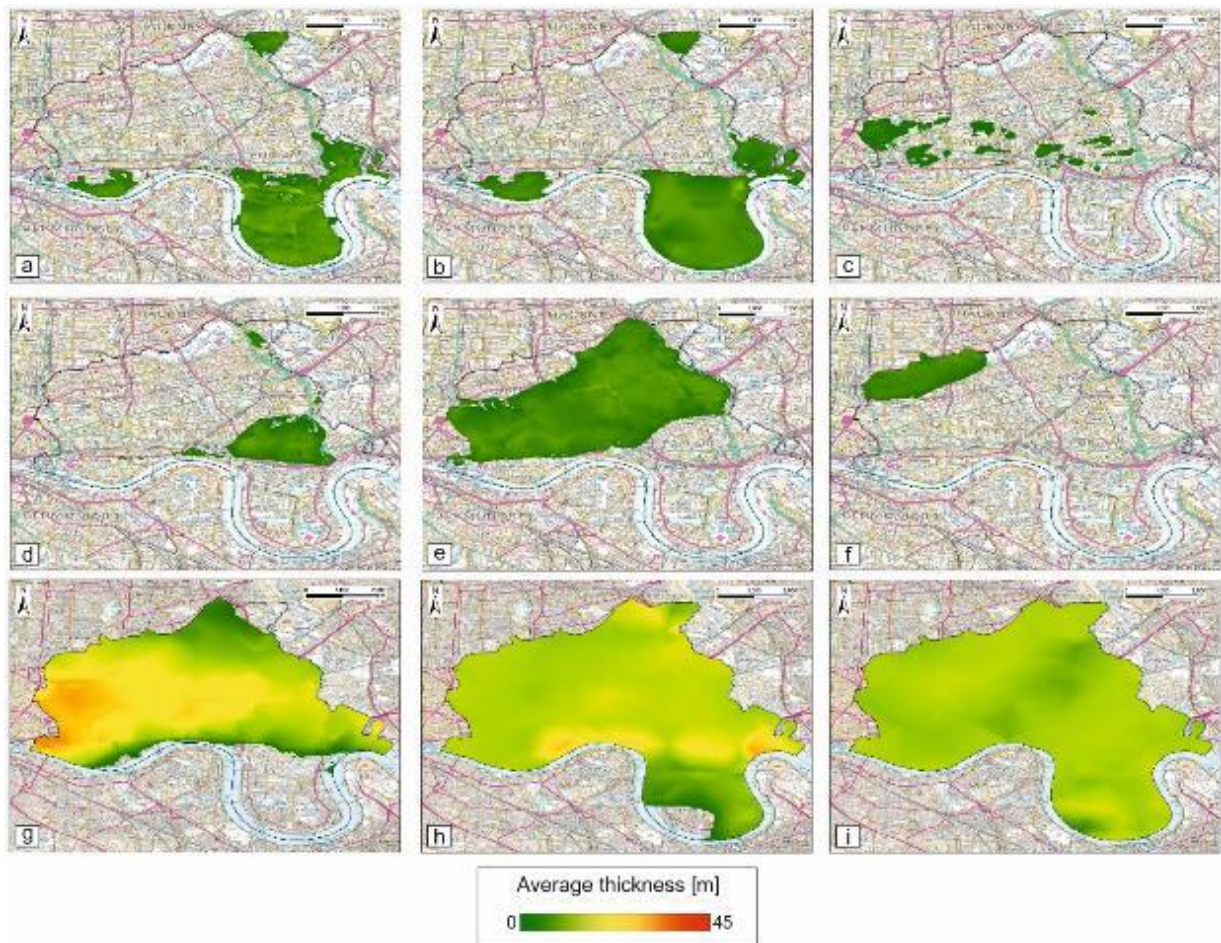


Figure 5. Thickness map in the AoI after removal of the AMG thickness (see Figure 2) for ALV (a), RTDU (b), LASI (c), KPGR (d), TPGR (e), HAGR (f), LC (g), LMBE (h) and TAB (i). Contains Ordnance Data © Crown Copyright and database rights 2019. Ordnance Survey Licence no. 100021290.

The AMG and the underlying units have then been individually compared in space and time with ground motion information derived from InSAR, in order to disentangle trends and patterns of the terrain displacement that can be connected to the underground geology. InSAR is a remote sensing technique allowing the measurement of ground deformation from the phase difference between SAR images acquired over the same area at different times by ground, air or space platforms (Rosen et al., 2000). This approach has proved to be particularly suitable solution for long term monitoring (>20 years) at a relative low cost and high precision especially in urban areas like London where intense exploitation of aquifers occurs and vertical movements might be significant (Bateson et al., 2009; Aldiss et al., 2014; Boni et al., 2018). The study has been performed combining data from 105 ascending and 111 descending SAR images acquired by Sentinel-1A/B satellites of the European Space Agency (ESA) between May 2015 to January 2018 with a nominal

revisit cycle of 6/12 days. The small spatial and temporal separation (baseline) between satellite orbits provided by Sentinel-1A/B reduces decorrelation noise effects (Zebker and Villasenor, 1992) affecting the interferograms and to maximize the number of reliable measurement points and is the reason why only this dataset has been considered among the ESA SAR data available in the last 25 years for the area.

Processing was carried out using the GAMMA software by CGG's NPA Satellite Mapping group within the framework of GIRP project (<https://business.esa.int/projects/girp>). Displacements are provided for 110 synthetic dates along the vertical direction resulting from the combination of the ascending and descending results for a total of 762,606 Measuring Points (MPs) minimally affected by temporal and geometric decorrelation over the Greater London Area (1,596 km² extended; Figure 6). Given an average standard deviation associated with the vertical velocity of ~1.5 mm/yr, a conservative velocity threshold of ± 5 mm/yr has been applied to consider a MP unstable.

In the investigated area, the coordinates of each MP can be expressed in term of X, Y, Z with the latter usually corresponding to radar reflection from building roofs. During integral analysis of the building deformation state, however, buildings usually can be considered as a rigid body without considering elastic deformation because they are made of reinforced concrete and a rigid motion model is sufficient to describe the deformation state of the whole structure (Yang et al., 2016). Under this assumption, the displacement information from the roof can be assimilated to the displacement information from the bottom of the building that could be either the ground surface or the sub-surface where its foundations lie.

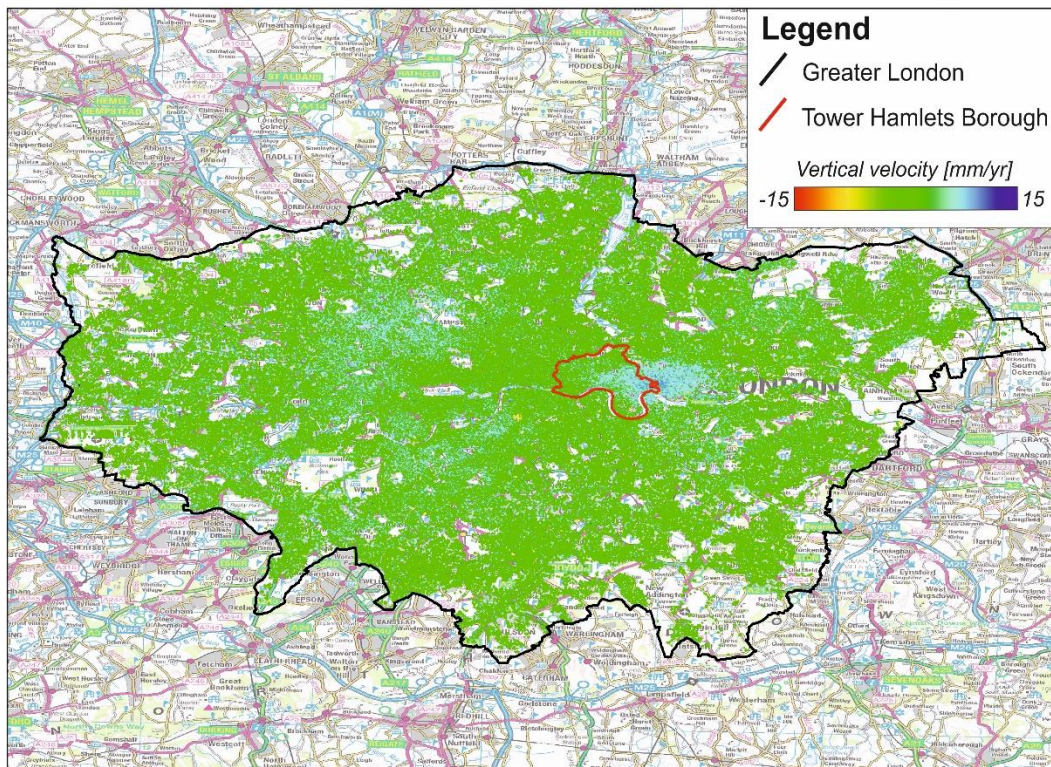


Figure 6. Vertical velocity measured by Sentinel-1 data during the period 2015 to 2018 across Greater London and the AOI (in red). Positive values indicate uplift and negative values indicate subsidence. InSAR data © CGG NPA Satellite Mapping 2018. Contains modified Copernicus Sentinel data 2014-2018. Contains Ordnance Data © Crown Copyright and database rights 2019. Ordnance Survey Licence no. 100021290.

The thickness of the AMG and the superficial and bedrock units has been analysed in connection to the 23,245 InSAR MPs within the AoI by considering two different semi-automatic ways of sorting MPs into groups that, in turns, could be correlated to the local geological or anthropogenic conditions:

1. MP average displacement rates.
2. Cluster analysis of the time series of the MP displacements.

Average displacement rates can represent an important clue especially when identifying linear patterns of motion like compaction of alluvial deposits but misleading when looking for shared patterns of deformation or when detecting non-linear or cyclic patterns of motion that have historically occurred in the Tower Hamlets area.

Clustering is one of the most common methods for unsupervised learning, where each data entry is given a cluster without any prior knowledge or input from the user.

The shape-based distance (SBD) clustering method was applied in the Tower Hamlets dataset as implemented in the k-shape algorithm (Paparrizos et al., 2015) from the R ‘dtwclust’ package (Sarda-Espinosa R., 2017). The Dynamic time warping Barycenter Averaging (DBA) method was used for the cluster’s centroid computation. With this process, the time series sequences are grouped into clusters where they have the most similar distance. Given x , y are two z -normalized time series subsequences and with m being their length, the shape-based distance (SBD) is calculated by the following equation:

$$SBD(\vec{x}, \vec{y}) = 1 - \max_w \left(\frac{CC_w(\vec{x}, \vec{y})}{\sqrt{R_0(\vec{x}, \vec{x}) \cdot R_0(\vec{y}, \vec{y})}} \right) \quad (1)$$

Where, CC_w is the cross-correlation in the position w , for each shift of x over time series y when x is slided by shifts $s \in [-m, m]$ and is computed by the formula:

$$CC_w(\vec{x}, \vec{y}) = R_{w-m}(\vec{x}, \vec{y}), \quad w \in \{1, 2, \dots, 2m - 1\} \quad (2)$$

Where R_s if $s=w-m$, is computed in turn, as:

$$R_s(\vec{x}, \vec{y}) = \begin{cases} \sum_{l=1}^{m-s} x_{l+s} \cdot y_l, & s \geq 0 \\ R_{-s}(\vec{y}, \vec{x}), & s < 0 \end{cases} \quad (3)$$

The goal of the process is to find the position w at which the cross-correlation maximizes equation (1). The SBD takes values between 0 and 2, where a value of 0 indicates perfect similarity between two time series x and y . The above process is performed k times, with k being the number of clusters. The clustering algorithm requires a single user parameter, k , to cluster the n time series observations (the satellite acquisitions in this case). However, because we do not know the number of clusters that exist in the dataset, an objective measure has to be used to find this optimal number $k < n$. A variety of cluster validity indices are used in the literature and in this work the elbow method was applied to decide the optimal number of clusters (Kodinariya et al., 2013). To find the “elbow”, the variance of the distribution represented by total sum of square (TSS) distances for each cluster has to be computed. In this case, for a set of clusters k , the TSS is computed by the function:

$$TSS = \sum_{i=1}^k SBD^2 \quad (4)$$

This calculation is performed for each different configuration of k-clusters and the TSS is plotted against the number of clusters. The algorithm is run several times because it returns a non-deterministic result with each experiment and as the number of clusters increases the TSS decreases and it will eventually become 0 if k becomes equal to the number of the time series sequences in the dataset.

The objective of this process is to find, either visually or by calculating the curvature, the number of clusters that resemble an “elbow” in the graph. The elbow point shows the highest drop in the TSS and means that the algorithm has achieved a well grouped clustering.

3 Results

InSAR data shows that the main deformation area is localised to a restricted area, $\sim 16 \text{ km}^2$, between Tower Hamlets and Newham London Boroughs.

Here, previous studies (Cigna et al., 2015) have shown that changes in groundwater management in the LMBE and TAB and engineering work in the ALV and AMG have been responsible for ground motions during the '90s and 2000s followed by the settlement, in the range between 3 mm and 30 mm, induced by the excavation activities of the Crossrail project (Benoît, 2010; Milillo et al., 2018). The latter is the largest underground excavation plan in Europe as of 2018 and encompasses the creation of 42 km twin-bore tunnels between 2012 and 2015 stretching from west to east London.

The end of the depressurisation activities in the TAB and the Chalk Group connected to the termination of the Crossrail project boring have been proven to be the cause of ground motions observed in the Sentinel-1 data (Bonì et al., 2018).

Despite most of the AoI being stable during the analysed time span, displacement rates up to 20 mm/yr characterize the Canary Warf area where KPGR, LC, LMBE and TAB occur (Figure 7) with only AMG and TAB overlapping with all the 23,245 MPs in the area (Table 2).

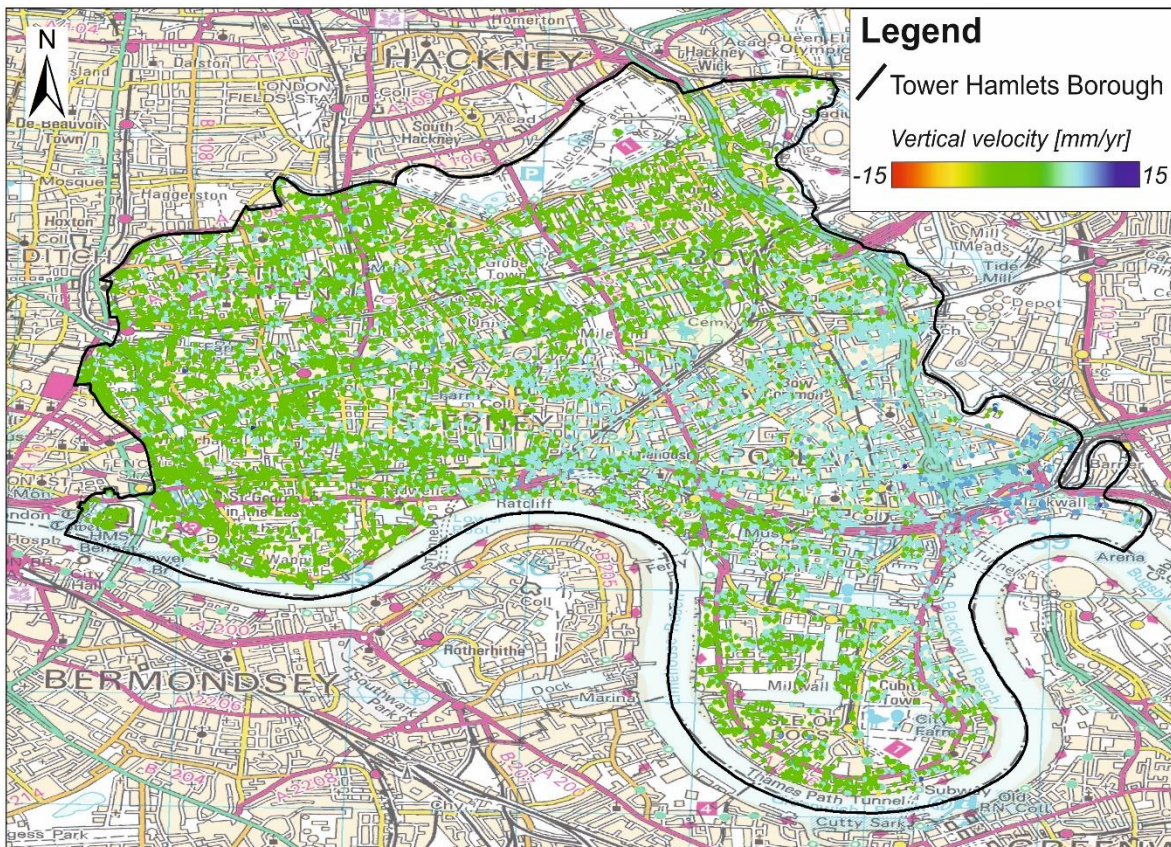


Figure 7. LOS velocity measured by Sentinel-1 data during the period 2015 to 2017 across Tower Hamlets (in black). Positive values indicate uplift and negative values indicate subsidence. InSAR data © CGG NPA Satellite Mapping 2019. Contains modified Copernicus Sentinel data 2014-2018. Contains Ordnance Data © Crown Copyright and database rights 2019. Ordnance Survey Licence no. 100021290.

Table 2. Number of MPs falling into each units ordered from the top to the bottom according to the local stratigraphy.

units	no of MPs
AMG	23,245
ALV	5,525
RTDU	5,610
LASI	2,241
KPGR	2,212
TPGR	12,484
HAGR	2,260
LC	19,578
LMBE	22,745
TAB	23,245

The density plots of Figure 8 shows the distribution between the average displacement motion of MPs and the underlying geology by considering the thickness of each superficial and bedrock unit along with AMG (Figure 8). All the correlation coefficients (ρ) between the variables are quite close to 0 with LASI, RTDU and especially LC showing a negative correlation.

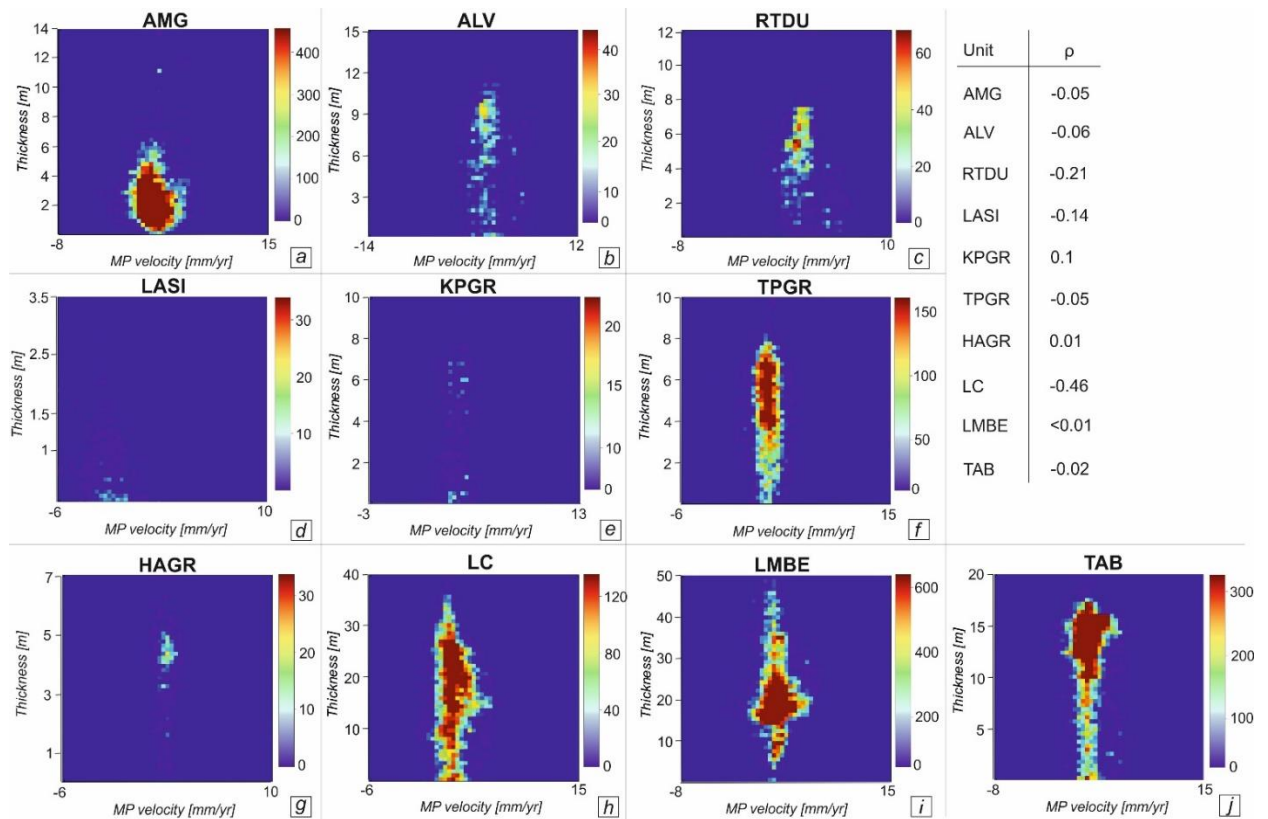


Figure 8. Comparison of MP average velocity with thickness of: AMG (a), ALV (b), RTDU (c), LASI (d), KPGR (e), TPGR (f), HAGR (g), LC (h), LMBE (i), TAB (j). The correlation coefficient values (ρ) are provided (top right).

The analysis continued by considering the comparison between the thickness of the units and the clusters with the number of clusters chosen according to the TSS as explained in section 2. We choose a number of clusters that account for the variance of the data, these are also clusters where the addition of a further cluster does not provide a better fit for the modelling of the data. At this point the marginal gain will drop, giving a strong curvature in the graph (Figure 9).

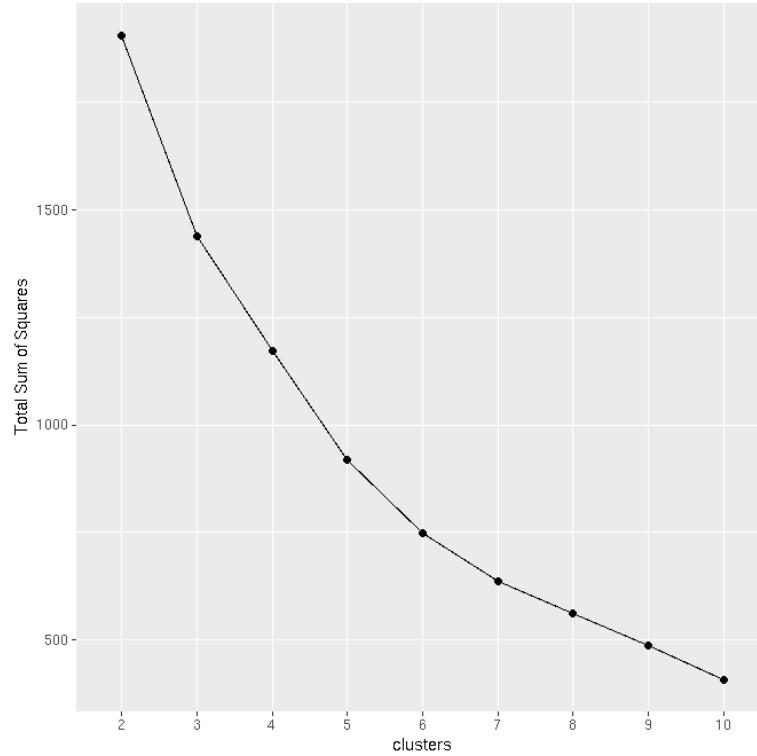


Figure 9. The elbow graph produced from clustering the Tower Hamlets dataset.

Calculating the second derivative will give us the curvature for each point at the graph. The second derivative results shown in Table 3, indicate that the best clusters k correspond to 3 and 5 classes. Even though the second derivative of cluster 3 is shown to be the best choice of clusters k , repeating the experiment with $k=3$ yields a very different clustering result. This problem is known to exist in imbalanced datasets with heavily under-sampled groups (Chawla, 2009). To be more precise, from the signals shown in Figure 10, group A represents the dominant signal in the area with 81.2% of MPs showing this pattern. Group B represents the 2.8%, group C the 1% and group D and E represent the 4.6% and 11.4% respectively. Because the majority of the groups are under-sampled, the second best choice of $k=5$ was selected as the number of groups. This choice is shown to represent the cluster distribution of the MPs better because the resulting groups retain their distinct features and shapes with low variation each time the algorithm runs. The results therefore can be regarded as consistent.

Table 3. The second derivative of each point from the graph shown in Figure 9.

<i>k</i> clusters	Second derivative
3	202.31
4	13.41
5	81.88
6	57.38
7	38.00
8	0.48
9	-4.92

In terms of temporal characteristics, groups A, C and D are within the ± 5 mm/yr threshold so, despite appearing slightly different, they all show overall stability. A and C both experience uplift, followed by stability and then a period of subsidence, whereas D does not experience the uplift at the start of the time series in 2015.

MPs classified as group B display a small linear subsidence trend over the 2 years period (Figure 10b). MPs in group E display a relatively rapid uplift in 2015 followed by a period of stability (Figure 10e).

V4

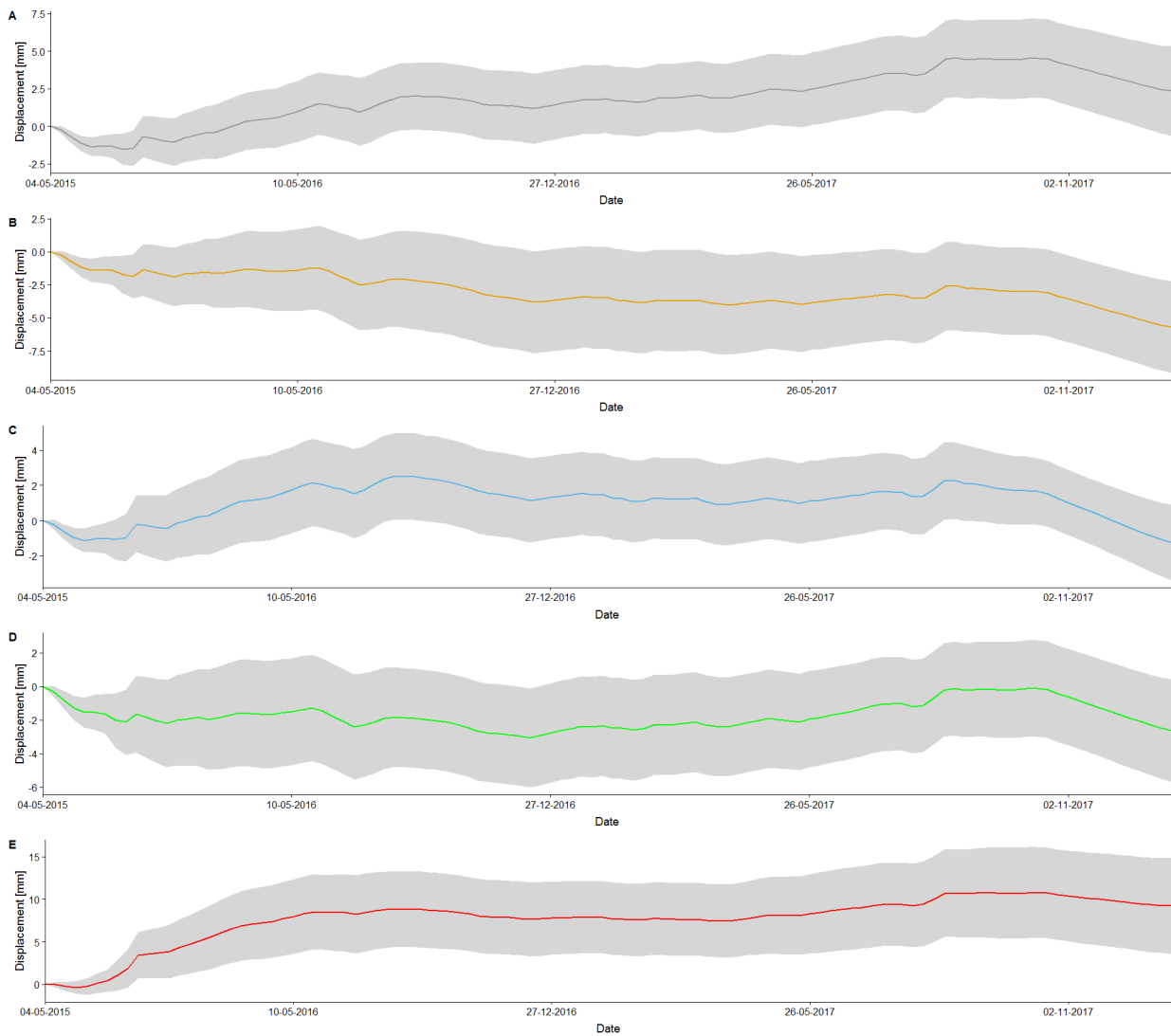


Figure 10. The spatial pattern of the shape-based distance cluster analysis. The solid curves show the centroids (median) of the distribution of the five clusters. The shaded area denotes the standard deviation ± 1 of each of the size bins, for all distributions that were members of the given clusters. Note the Y-axis has been scaled for each plot independently to highlight the differences within the plot.

Considering the number of MPs within each group, group A is always dominant over the others groups in every unit and, overall, the number of MPs in each cluster group does not relate to the occurrence of specific units (Figure 11). However, group E represents a consistent portion in ALV with 27% of the total number of MPs for this unit (Figure 11b) compared to an average of 10.8% of MPs belonging to group E for the other layers (Figure 11).

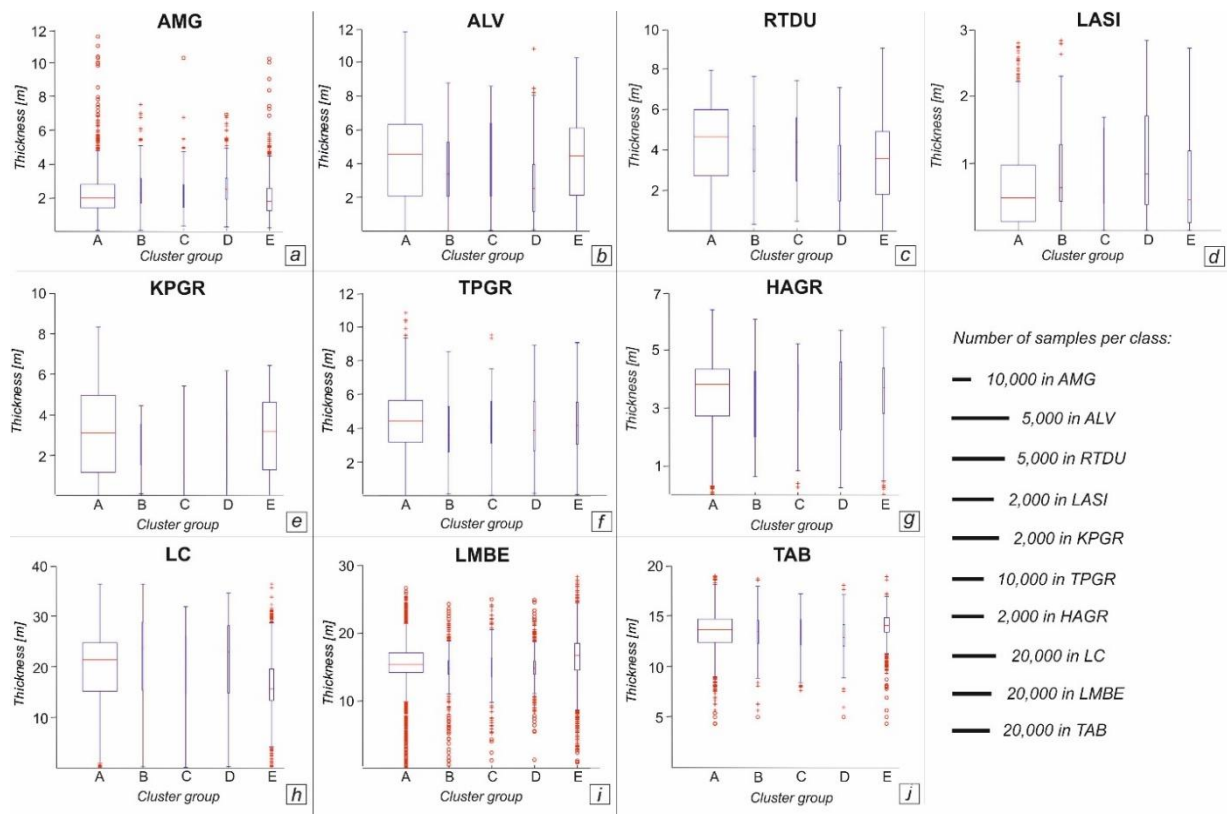


Figure 11. Comparison of clustering trends with thickness of: AMG (a), ALV (b), RTDU (c), LASI (d), KPGR (e), TPGR (f), HAGR (g), LC (h), LMBE (i), TAB (j). On each box, the central mark indicates the median, and the bottom and top edges of the box indicate the 25th and 75th percentiles, respectively. The whiskers extend to the most extreme data points not considering outliers. Outliers are plotted using the red '+' symbol if they lie between 1.5 and 3 times the interquartile range or the red 'o' symbol if they lie outside 3 times the interquartile range. Box width is proportional to the number of samples within each cluster.

By considering the median and the Interquartile Range (IQR) values of the normalised distributions, the percentile analysis of the boxplots of Figure 11 has been performed in order to assess the relationship between the thickness and the cluster groups within each units (i.e., the colours in Figure 12) and among the different units (i.e., the symbols in Figure 12). The lack of a dispersion of the cluster groups within the same unit, in particular for LMBE and TAB, confirm the absence of correlation between the groups and the thickness. On the other hand, there appears to be a slight negative correlation between IQR and the median values for the each cluster group across the different units, however the confidence in the correlation is low because of the large spread in the data.

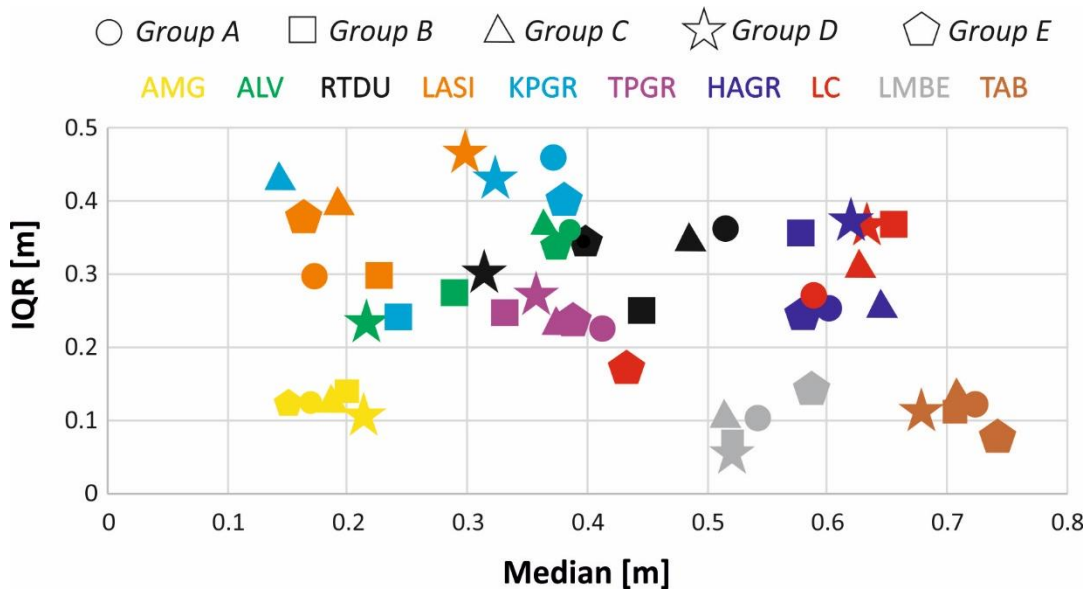


Figure 12. Distribution of median and IQR values of the cluster groups for each unit, after the normalization of the thickness values.

The majority of MPs are classified into group A and therefore assessed to be stable with the eastern side of Tower Hamlets dominated by group E (Figure 13a). Group D is mainly associated with two structures: Old Spitalfields Market and Tobacco Dock. MPs assigned to groups B and C appear to be not connected in space and therefore isolated from other MPs belonging to that group.

Temporally and spatially, group E can be straightforwardly connected with the rising groundwater level, up to 20 m, in the deep and confined aquifer of the TAB and the Chalk Group (Figure 13b) following the end of the bulk of Crossrail dewatering activities in the area from August 2015 (Crossrail, 2016). It should be noted that, with the termination of Crossrail dewatering, the drawdown effect induced by Crossrail has now fully dissipated and that the dewatering works have complied with the obligations as enshrined in Section 46 of the Crossrail Act (2008), available at: <https://www.legislation.gov.uk/ukpga/2008/18/contents>.

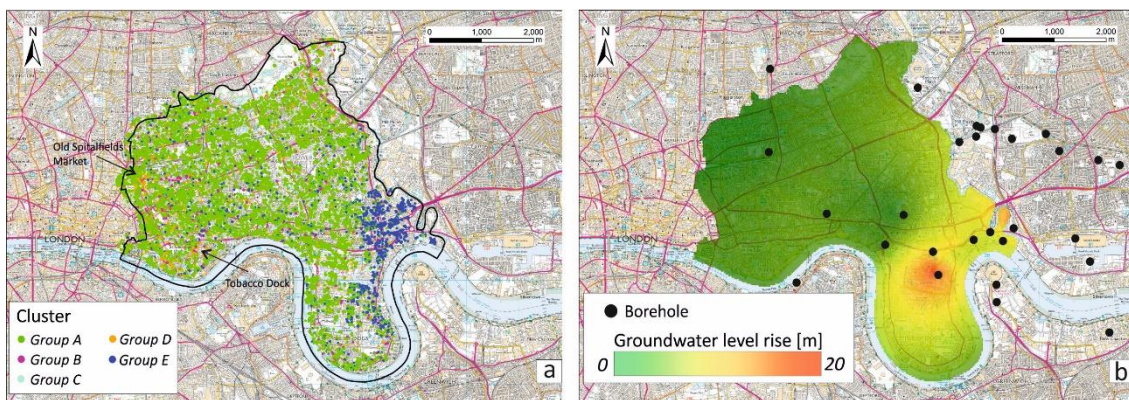


Figure 13. Distribution of clustering groups in Tower Hamlets area (a) and groundwater level increase between August 2015 and May 2016 (b). Borehole data used for interpolating the groundwater levels have been provided with the permissions of Canary Wharf Contractors, Crossrail Ltd, Environment Agency and Thames Water. These reproduced materials are courtesy of Crossrail Ltd. Contains Ordnance Data © Crown Copyright and database rights 2019. Ordnance Survey Licence no. 100021290.

4 Discussion and Conclusions

With the recent surge in the availability of free SAR data, millions of measurement points are routinely being generated with short revisiting time. There is therefore a need to develop methodologies to understand the complexity of the components within the time series of the data. The clustering analysis used within this study is one such methodology upon which new case studies can be developed and new insights can be generated.

In particular, by exploiting the high temporal density of InSAR displacement data, this study illustrates how average displacement rates and cluster analysis can be used to investigate the characteristics of the human-induced deformation in the Tower Hamlets area and the relationships with the thickness map of the local geological units.

According to our results, ALV is the unit that is mostly affected by the deformation as proven by the relatively large number of MPs classified in to group E but, overall, the cluster groups we identified do not have correlation with the thickness of the units. In particular, no correlations between the AMG thickness and the MPs deformation has been found, probably because the foundation depth of the buildings in this area lie well below its lowest occurrence so these buildings tend to respond to strains affecting a deeper source rather than the top layer.

We can then conclude that the thickness of the lithological units directly above the Chalk Group does not have overall influence in the ground deformation behaviour.

Our first results for the Tower Hamlets area show also that the analysis of the average motion alone is not a good indicator for highlighting any influence between the unit thickness and ground motion because of:

- the short time interval considered, which does not allow the recognition of large temporal trends such as compaction of unconsolidated deposits.
- The narrow range of deformation and the small area of study, the latter limited by the availability of the new 3D geological model, that does not allow to encompass the whole area of uplift which extends eastwards (see Figure 6) and to extend our conclusion to the whole Greater London area.

Therefore, further work may be considered in order to spatially and temporally extend our analysis (i), to account for the actual saturated thickness of the layers above the Chalk Group (e.g., LC and LMBE; ii) and to consider the impact of urban features (e.g., building type, building age; iii) that show local patterns of subsidence (Old Spitalfields Market and Tobacco Dock) almost impossible to be detected without the clustering analysis.

The results presented here, although not conclusive, do show the huge potential of clustering analysis in analysing large matrix generated by InSAR data for displacement pattern recognition and in highlighting the strong influence of dewatering activities on ground deformation, thus providing more easy-to-interpret data to stakeholders (e.g., engineering consultants) or public organisations that are in charge of coordinate urban policies and hazard mitigation strategies.

5 Acknowledgments

The authors would like to acknowledge B.P. Marchant for the fruitful discussions, © CGG NPA Satellite Mapping who generated the InSAR results and the ESA Copernicus programme who provided access to the Sentinel-1 data.

References

- ALDISS, D T, BLACK, M G, ENTWISLE, D C, PAGE, D P AND TERRINGTON, R L, 2012. Benefits of a 3D geological model for major tunnelling works: an example from Farringdon, east-central London, UK. *Geological Society of London*. <https://doi.org/10.1144/qjgegh2011-066>
- ALDISS, D, BURKE, H, CHACKSFIELD, B, BINGLEY, R, TEFERLE, N, WILLIAMS, S, BLACKMAN, D, BURREN, R AND PRESS, N. 2014. Geological interpretation of current subsidence and uplift in the London area; UK, as shown by high precision satellite-based surveying. *Proc. Geol. Assoc.*, 125. 1–13. <https://doi.org/10.1016/j.pgeola.2013.07.003>
- BATESON, L B, BARKWITH, A K A P, HUGHES, A, G AND ALDISS, D T. 2009. Terrafirma: London H-3 Modelled Product: Comparison of PS Data with the Results of a Groundwater Abstraction Related Subsidence Model. *British Geological Survey Commissioned Report OR/09/032*. <http://nora.nerc.ac.uk/id/eprint/8581/1/OR09032.pdf>
- BENOIT, J., 2010. Low-volume-loss tunnelling for London ring main extension. *Proceedings of the ICE - Geotechnical Engineering*, 163 (3). doi:10.1680/geng.2010.163.3.167
- BERTI, M, CORSINI, A, FRANCESCHINI, S AND IANNAONE, J P. 2013. Automated classification of Persistent Scatterers Interferometry time series. *Nat Hazard Earth Sys*, 13(8). 1945–1958. <https://doi.org/10.5194/nhess-13-1945-2013>
- BONI, R, BOSINO, A, MEISINA, C, NOVELLINO, A, BATESON, L AND MCCORMACK, H. 2018. A Methodology to Detect and Characterize Uplift Phenomena in Urban Areas Using Sentinel-1 Data. *Remote Sensing*, 10(607). <https://doi.org/10.3390/rs10040607>
- BRIDGE, D M, BUTCHER, A, HOUGH, E, KESSLER, H, LELLIOTT, M, PRICE, S J, REEVES, H J, TYE, A M, WILDMAN, G, AND BROWN, S. 2010. Ground conditions in central Manchester and Salford: the use of the 3D geoscientific model as a basis for decision support in the built environment. *British Geological Survey Research Report* <http://nora.nerc.ac.uk/id/eprint/16120/1/RR10006.pdf>
- BRIDGE, D M, HOUGH, E, KESSLER, H, PRICE, S J AND REEVES, H. 2005. Urban geology: integrating surface and sub-surface geoscientific information for developing needs. 129–134. In: Ostaficzuk S.R. (eds) *The Current Role of Geological Mapping in Geosciences*. NATO Science Series (Series IV: Earth and Environmental Sciences), 56. Springer, Dordrecht.
- BURKE, H F, MATHERS, S J, WILLIAMSON, J P, THORPE, S, FORD, J R AND TERRINGTON, R L. 2014. The London Basin superficial and bedrock LithoFrame 50 Model. *British Geological Survey Open Report* OR/14/029. http://nora.nerc.ac.uk/id/eprint/507607/1/London_Basin_Superficial_and_Bedrock_Lith50_OR_14_029.pdf
- CHAWLA, N V. 2009. Data mining for imbalanced datasets: An overview. In *Data mining and knowledge discovery handbook*. Springer, Boston, MA, 875–886.
- CIGNA, F, JORDAN, H, BATESON, L, MCCORMACK, H AND ROBERTS, C. 2015. Natural and Anthropogenic Geohazards in Greater London Observed from Geological and ERS-1/2 and ENVISAT Persistent Scatterers Ground Motion Data: Results from the EC FP7-SPACE PanGeo Project. *Pure Appl. Geophys.* 172, 2965–2995. <https://doi.org/10.1007/s00024-014-0927-3>
- CROSSRAIL, 2016. Crossrail Project Dewatering Works—Close-out Report. Available online: https://learninglegacy.crossrail.co.uk/wp-content/uploads/2017/01/7A-026_1-Dewatering-Close-out-report.pdf (accessed on 12 November 2017).
- ENVIRONMENT AGENCY, 2018. Management of the London Basin Chalk Aquifer; Status Report 2018. Available online at: <https://www.gov.uk/government/publications/london-basin-chalk-aquifer-annual-status-report> (accessed on 16 November 2018).
- FORD, J R, PRICE, S J, COOPER, A H, AND WATERS, C N. 2014. An assessment of lithostratigraphy for anthropogenic deposits. *Geological Society, London, Special Publications*, 55–89.
- KESSLER, H, MATHERS, S J AND SOBISCH, H G. 2009. The capture and dissemination of integrated 3D geospatial knowledge at the British Geological Survey using GSI3D software and methodology. *Computers and Geosciences*, 35, 1311–1321.
- KESSLER, H AND MATHERS, S J. 2004. From geological maps to models – finally capturing the geologists’ vision. *Geoscientist*, 14/10, 4–6.
- KODINARIYA, T M AND MAKWANA, P R. 2013. Review on determining number of Cluster in K-Means Clustering. *International Journal*, 1(6), pp.90–95.
- JONES, L D AND TERRINGTON, R. 2011. Modelling modelling volume change potential in the London Clay. *Quarterly Journal of Engineering Geology and Hydrogeology*, 44 (1), 109–122. <https://doi.org/10.1144/1470-9236/08-112>.
- MILILLO, P, GIARDINA, G, DEJONG, M J, PERISSIN, D AND MILILLO, G. 2018. Multi-Temporal InSAR Structural Damage Assessment: The London Crossrail Case Study. *Remote Sensing*, 10(2). 287. <https://doi.org/10.3390/rs10020287>
- NOVELLINO, A, CIGNA, F, BRAHMI, M, SOWTER, A, BATESON, L AND MARSH, S. 2017. Assessing the feasibility of a National InSAR Ground Deformation Map of Great Britain with Sentinel-1. *Geosciences*, 7(2). <https://doi.org/10.3390/geosciences7020019>
- PAPARRIZOS, J. AND Gravano, L., 2015. k-shape: Efficient and accurate clustering of time series. In *Proceedings of the 2015 ACM SIGMOD International Conference on Management of Data* (pp. 1855–1870). ACM.
- PRICE, S J, TERRINGTON, R L, BURKE, H F, SMITH, H, AND THORPE, S. 2012. Anthropogenic Landscape evolution and modelling of artificial ground in urban environments: case studies from central London, UK. *British Geological Survey Open Report* OR/15/010. <http://nora.nerc.ac.uk/id/eprint/510140/1/OR15010.pdf>

- ROSEN, P A, HENSLEY, S, JOUGHIN, I R, LI, F K, MADSEN, S N, RODRIGUEZ, E AND GOLDSTEIN, R M. 2000. Synthetic Aperture Radar Interferometry. *Proceedings of the IEEE*, 88(3), 333-382.
- SARDA-ESPINOSA, A., 2017. Comparing time-series clustering algorithms in r using the dtwclust package. *R package vignette*, 12.
- TERRINGTON, R L, THORPE, S, BURKE, H F, SMITH, H AND PRICE, S J. 2015. ENHANCED MAPPING OF ARTIFICIALLY MODIFIED GROUND IN URBAN AREAS : USING BOREHOLE, MAP AND REMOTELY SENSED DATA. NOTTINGHAM, UK, BRITISH GEOLOGICAL SURVEY, 38PP.
- TERRINGTON, R. L., SILVA, É CN, WATERS, C N, SMITH H AND THORPE, S., 2018. Quantifying anthropogenic modification of the shallow geosphere in central London, UK. *Geomorphology*, 319. 15-34. <https://doi.org/10.1016/j.geomorph.2018.07.005>
- YANG, K., YAN, L., HUANG, G., CHEN, C., AND WU, Z. 2016. Monitoring building deformation with InSAR: Experiments and validation. *Sensors*, 16(12). <https://doi.org/10.3390/s16122182>
- ZALASIEWICZ, J, WATERS, C N, DO SUL, J A I, CORCORAN, P L, BARNOSKY, A D, CEARRETA, A, EDGEWORTH, M, GALUSZKA, A, JEANDEL, C, LEINFELDER, R AND MCNEILL, J R. 2016. The geological cycle of plastics and their use as a stratigraphic indicator of the Anthropocene. *Anthropocene*, 13. 4-17. <https://doi.org/10.1016/j.ancene.2016.01.002>
- ZALASIEWICZ, J, WILLIAMS, M, HAYWOOD, A, AND ELLIS, M. 2011. The Anthropocene: a new epoch of geological time?. *Philosophical Transactions of the Royal Society A*, 369. 835-841. <https://doi.org/10.1098/rsta.2010.0339>
- ZEBKER, H A AND VILLASENOR, J. 1992. Decorrelation in interferometric radar echoes *IEEE Trans. Geosci. Remote Sens.*, 30 (5). 950-959.